Cytokinin Response Factor 6 Represses Cytokinin-Associated Genes during Oxidative Stress[1][OPEN]

Paul J. Zwack, Inge De Clercq, Timothy C. Howton, H. Tucker Hallmark, Andrej Hurny, Erika A. Keshishian, Alyssa M. Parish, Eva Benkova, M. Shahid Mukhtar, Frank Van Breusegem, and Aaron M. Rashotte*

Department of Biological Sciences, Auburn University, Auburn, AL 36849 (P.J.Z., H.T.H., E.A.K., A.M.P., A.M.R.); Department of Plant Systems Biology, VIB, 9052 Ghent, Belgium (I.D.C., F.V.B.); Department of Plant Biotechnology and Bioinformatics, Ghent University, Technologiepark 927, B-9052 Gent, Belgium (I.D.C., F.V.B.); Department of Biology, University of Alabama, Birmingham, AL 35294 (T.C.H., M.S.M.); and Institute of Science and Technology Austria (IST Austria), 3400 Klosterneuburg, Austria (A.H., E.B.)

ORCID IDs: 0000-0003-3477-9043 (P.J.Z.); 0000-0001-8125-1239 (I.D.C.); 0000-0003-3638-1426 (A.H.); 0000-0002-3147-0860 (F.V.B.); 0000-0001-5034-4395 (A.M.R.).

Cytokinin is a phytohormone that is well known for its roles in numerous plant growth and developmental processes, yet it has also been linked to abiotic stress response in a less defined manner. Arabidopsis (*Arabidopsis thaliana*) Cytokinin Response Factor 6 (CRF6) is a cytokinin-responsive AP2/ERF-family transcription factor that, through the cytokinin signaling pathway, plays a key role in the inhibition of dark-induced senescence. CRF6 expression is also induced by oxidative stress, and here we show a novel function for CRF6 in relation to oxidative stress and identify downstream transcriptional targets of CRF6 that are repressed in response to oxidative stress. Analysis of transcriptomic changes in wild-type and *crf6* mutant plants treated with H_2O_2 identified CRF6-dependent differentially expressed transcripts, many of which were repressed rather than induced. Moreover, many repressed genes also show decreased expression in 35S:CRF6 overexpressing plants. Together, these findings suggest that CRF6 functions largely as a transcriptional repressor. Interestingly, among the H_2O_2 repressed CRF6-dependent transcripts was a set of five genes associated with cytokinin processes: (signaling) ARR6, ARR9, ARR11, (biosynthesis) LOG7, and (transport) ABCG14. We have examined mutants of these cytokinin-associated target genes to reveal novel connections to oxidative stress. Further examination of CRF6-DNA interactions indicated that CRF6 may regulate its targets both directly and indirectly. Together, this shows that CRF6 functions during oxidative stress as a negative regulator to control this cytokinin-associated module of CRF6-dependent genes and establishes a novel connection between cytokinin and oxidative stress response.

The frequent environmental changes to which a plant is subject can lead to physiological alterations and disruption of normal metabolism. In particular, the energetic reactions that take place in chloroplasts, peroxisomes, and mitochondria are susceptible to dysfunction, which results in production of excessive levels of reactive oxygen species (ROS). In fact, many common abiotic stress conditions encountered in agriculture, including temperature extremes, drought, soil salinity, and air pollution, are known to include an oxidative stress component (Gill and Tuteja, 2010). Cellular levels of ROS are carefully maintained at relatively low levels through a wide range of scavenging and detoxification mechanisms. However, if the balance between ROS production and removal is shifted too far toward production (e.g. under stress conditions), cellular damage can occur as a result of oxidation of macromolecules such as lipids, proteins, and nucleic acids (Mittler, 2002; Gill and Tuteja, 2010). Accumulation of ROS beyond some threshold triggers cell death as a response. Therefore, ROS are thought to serve as indicators of oxidative stress within a cell but may also

[1] This work was financially supported by the following: The Alabama Agricultural Experiment Station HATCH grants 370222-310010-2055 and 370225-310006-2055 for funding to P.J.Z., E.A.K, A.M.P., and A.M.R. P.J.Z. and E.A.K were supported by an Auburn University Cellular and Molecular Biosciences Research Fellowship. I.D.C. is a postdoctoral fellow of the Research Foundation Flanders (FWO) (FWO/PDO14/043) and is also supported by FWO travel grant 12N2415N. F.V.B. was supported by grants from the Interuniversity Attraction Poles Programme (IUAP P7/29 MARS) initiated by the Belgian Science Policy Office and Ghent University (Multidisciplinary Research Partnership Biotechnology for a Sustainable Economy, grant 01MRB510W).

* Address correspondence to rashotte@auburn.edu.

The author responsible for distribution of materials integral to the findings presented in this article in accordance with the policy described in the Instructions for Authors (www.plantphysiol.org) is: Aaron M. Rashotte (rashotte@auburn.edu).

P.J.Z., I.D.C., E.V., M.S.M., F.V.B., and A.M.R. designed research; P.J.Z., I.D.C., H.T.H., A.H., E.A.K., A.M.P., E.B., T.C.H., M.S.M., F.V.B., and A.M.R performed research and analyzed data; P.J.Z. and A.M.R. wrote the paper.

[OPEN] Articles can be viewed without a subscription.

www.plantphysiol.org/cgi/doi/10.1104/pp.16.00415

Downloaded from www.plantphysiol.org on October 10, 2016 - Published by www.plantphysiol.org
Copyright © 2016 American Society of Plant Biologists. All rights reserved.

play a role in systemic stress signaling, as defined elsewhere (Petrov and Van Breusegem, 2012; Wrzaczek et al., 2013; Suzuki et al., 2012).

Phytohormones also play important roles in stress response signaling (O'Brien and Benková, 2013). One such hormone, cytokinin, is generally considered to be an antagonist of stress tolerance (Argueso et al., 2009; Ha et al., 2012; Zwack and Rashotte, 2015; Nguyen et al., 2016). In Arabidopsis (*Arabidopsis thaliana*), reduced cytokinin levels as a result of decreased synthesis or increased degradation have been found to increase tolerance to drought stress (Nishiyama et al., 2011; Macková et al., 2013). Compromised cytokinin signaling in mutants of various components of the cytokinin signaling pathway enhance drought, salt, and freeze tolerance (Tran et al., 2007; Jeon et al., 2010; Mason et al., 2010). Each of these conditions is known to stimulate ROS production; however, oxidative stress has not been directly examined in these mutants.

CYTOKININ RESPONSE FACTORS (CRFs) are a subset of the plant specific AP2/ERF domain-containing transcription factor family that function both downstream, and as a side branch, of the primary cytokinin signaling pathway (Rashotte et al., 2006; Cutcliffe et al., 2011). Arabidopsis *CRF6* is transcriptionally induced by cytokinin and plays a role in delaying leaf senescence (Zwack et al., 2013). *CRF6* expression is also induced in response to a wide range of stress stimuli, including oxidative stress in the form of both treatment with and endogenous production of H_2O_2 (Zwack et al., 2013; Inzé et al., 2012). In addition, *CRF6* is a direct target of retrograde signaling in response to organellar dysfunction (De Clercq et al., 2013; Ng et al., 2013). As such, this transcription factor has been proposed to integrate cytokinin and stress responses as part of a finely tuned response network (Zwack et al., 2013).

Here, we demonstrate that CRF6 functions in mediating the response to oxidative stress, in part through the repression of a set of genes involved in cytokinin metabolism, transport, and signaling. Thus, we propose that CRF6 acts to attenuate cytokinin signaling as part of an adaptive response to stress.

RESULTS

Increased Expression of CRF6 Alters Response to Oxidative Stress

Expression of *CRF6* is induced in response to a wide range of stress-associated conditions; therefore, we examined whether increased expression of *CRF6* could alter oxidative stress response. *CRF6* overexpression lines (*35S:CRF6*, denoted as *CRF6oe*) were generated, and phenotypes were observed under a range of oxidative stress conditions. Individual leaves excised from transgenic (CRF6oe) and azygous plants (wild type) were floated for 24 h on a solution containing either 20 mM H_2O_2 as an exogenous treatment or 10 mM 3-amino-1,2,4-triazole (3-AT), which inhibits catalase activity, resulting in an accumulation of endogenously produced H_2O_2. The maximal PSII quantum efficiency (F_v/F_m) of individual leaves was examined to determine the effect of these oxidative stress treatments on photosynthetic parameters (Fig. 1; Supplementary Fig. S1; Baker, 2008). Interestingly, the average F_v/F_m of wild-type leaves (0.82) was significantly greater than that of CRF6oe leaves (0.78) prior to treatment (Fig. 1A). However, the reduction in F_v/F_m after oxidative stress treatments was significantly different for the two genotypes, where the average F_v/F_m of CRF6oe leaves was greater (0.75 and 0.60, respectively for H_2O_2 and 3-AT) than leaves of wild type (0.72 and 0.53; two-way ANOVA $P = 0.0002$; Fig. 1A).

We further examined the effects of overexpression of *CRF6* using a bioassay in which gas exchange was restricted (restricted gas [RG]) to increase photorespiratory-dependent H_2O_2 accumulation (see "Methods" for details. Similar F_v/F_m levels were observed for leaves of intact dark-adapted wild-type (0.75) and CRF6oe (0.76) plants (as opposed to excised leaves as in Fig. 1A) under standard in vitro growth conditions. However, after 4 d of RG stress, the average F_v/F_m was higher in CRF6oe (0.67) compared to wild type (0.61; Fig. 1, B and C; Supplementary Fig. S1A). We also measured the operating PSII efficiency (ΦII) during a time course following exposure to normal actinic light and found that ΦII was significantly greater for CRF6oe plants under standard and RG conditions (Supplemental Fig. S1). ΦII can be broken down into its F_v'/F_m' and qP components (Genty et al., 1989), and a stronger increase in the efficiency of excitation energy transfer to the reaction centers that are open (F_v'/F_m') was observed for CRF6oe under stress conditions (Fig. 1E). Accordingly, we also observed lower heat produced as a result of dissipation of excitation energy (nonphotochemical quenching [NPQ]) for CRF6oe plants in a stress-specific manner (Fig. 1F). Under these conditions, we did not observe significant differences in any nondark adapted parameters for *crf6* loss-of-function mutant plants. Nonetheless, the altered response to both exogenous treatment with and endogenous production of H_2O_2 demonstrated for plants overexpressing *CRF6*, along with the previously reported transcriptional regulation of *CRF6* under oxidative stress conditions, suggests that this transcription factor plays a key role in the response to ROS, in particular to H_2O_2. Furthermore, to determine if CRF6 could affect responses to oxidative stress in different aspects of plant growth, root growth was examined in altered CRF6 expression lines in the presence and absence of antimycin A (AA), which interferes with the respiratory electron transport chain leading to the accumulation of ROS (Fig. 1D). Wild-type plants show a significant ($P < 0.001$) decrease in root growth to only 35% of untreated controls after AA treatment. CRF6oe roots were significantly ($P < 0.01$) less affected than wild type, whereas the knockout mutant *crf6-2* showed the opposite and was more ($P < 0.05$) affected (Fig. 1D).

Downloaded from www.plantphysiol.org on October 10, 2016 - Published by www.plantphysiol.org
Copyright © 2016 American Society of Plant Biologists. All rights reserved.

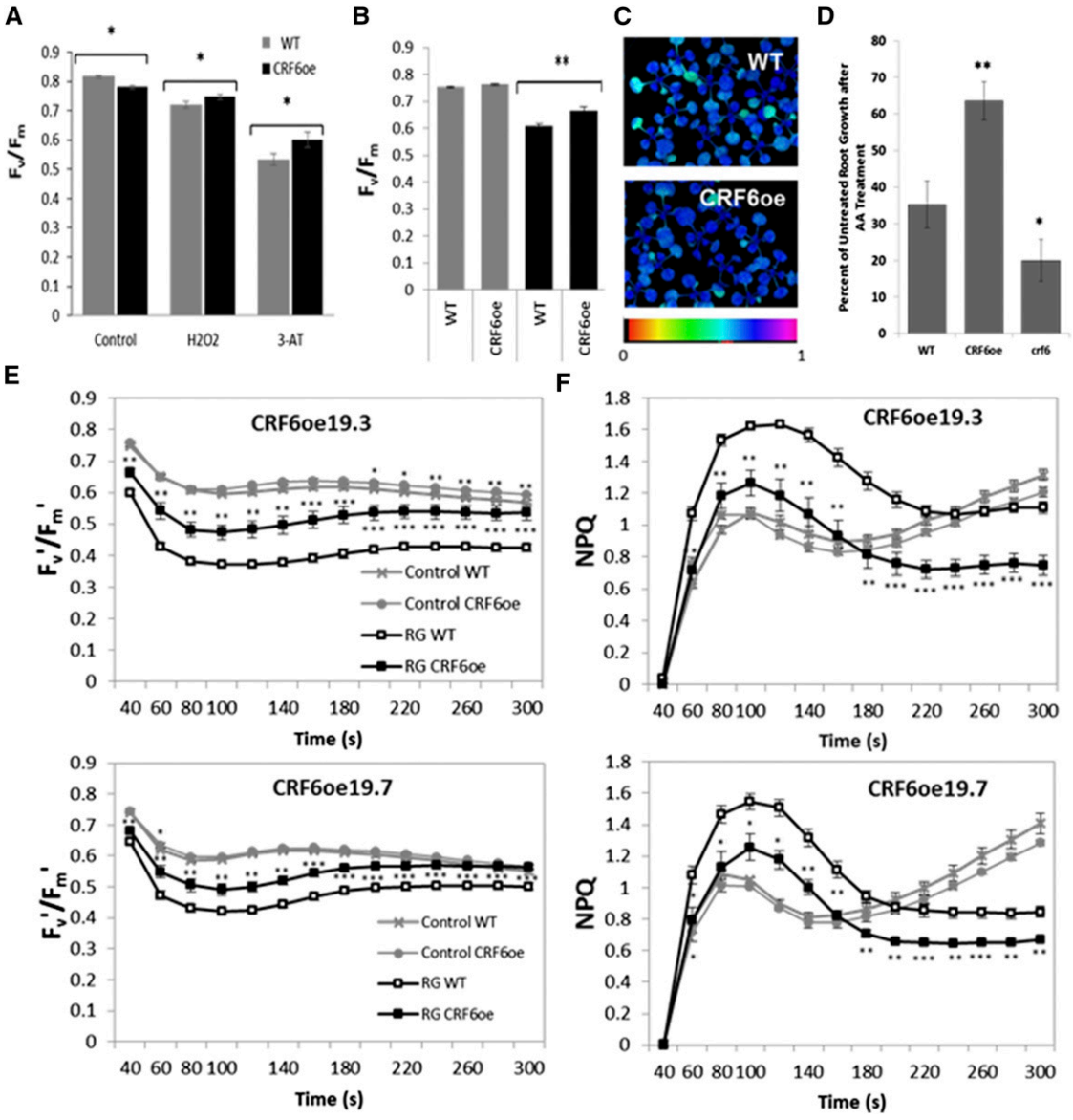

Figure 1. Overexpression of CRF6 affects alterations in chlorophyll fluorescence parameters induced by oxidative stress. A, Maximum PSII F_V/F_M of excised leaves before and 24 h after treatment with 20 mM H_2O_2 or 10 mM 3-AT. B, F_V/F_M of leaves of intact plants exposed to either normal growth conditions (control) or photorespiratory-induced oxidative stress conditions (RG). C, False-color heat map image of plants from B showing differences across plants. After determination of F_V/F_M followed by 40 s of darkness, plants were exposed to actinic light, and maximum and steady-state fluorescence were determined every 20 s for 5 min. F'_V/F'_M, *E*, NPQ *F*, PSII operating efficiency, and φ_{PSII} and qP (Supplemental Fig. S1) were calculated. D, Primary root growth (from day 4 to 9) under oxidative stress (5 mM AA) relative to untreated growth control for the given genotypes. Data points represent the mean ± SEM of $n \geq 8$ leaves for treatments and $n \geq 5$ leaves for controls, and $n \geq 10$ for roots from three independent experiments. Significance determined by Student's *t* test; $^*P < 0.05$, $^{**}P < 0.01$, $^{***}P < 0.001$.

CRF6 Partially Mediates Transcriptional Response to H_2O_2

We hypothesized that as a transcription factor, CRF6 may regulate oxidative stress response by regulating the expression of certain genes as part of a genome-wide transcriptional reprogramming. To test this, we examined global transcriptome changes in response to H_2O_2 (20 mM) treatment after 6 h in 10-d-old wild-type and *crf6* loss-of-function mutant plants by microarray analysis (Supplementary Dataset S1). Levels of 956 transcripts (606 induced and 351 repressed; fold change >2, adj. $P < 0.05$) were altered by H_2O_2 in wild type. Analysis of functional annotations associated with these transcripts indicated that the Gene Ontogeny (GO) terms "response to oxidative stress" and "response to hydrogen peroxide" were enriched with the highest confidence scores (Benjamini Hochberg, P = 3.2E-18 and 9.5E-18, respectively), indicating that the

Downloaded from www.plantphysiol.org on October 10, 2016 - Published by www.plantphysiol.org
Copyright © 2016 American Society of Plant Biologists. All rights reserved.

treatment had the intended effects on overall expression patterns. When we examined the expression of these oxidative stress-regulated genes under identical conditions in the *crf6* mutant background, we found that a subset (147 or 15%) was regulated in a CRF6-dependent manner (having a >50% decrease in magnitude of fold change compared to the wild-type background; Fig. 2A). While only 49 (8.1%) of the oxidative stress-induced genes were CRF6 dependent (Supplemental Table S1), 98 of the 351 (28%) genes repressed in wild type showed CRF6 dependence (Supplemental Table S2). This bias suggests that CRF6 plays a larger role in repressing the expression of genes in response to oxidative stress. Importantly, we found the expression of 132 transcripts to be altered in *crf6* under control conditions, yet these included only 6 CRF6-dependent-induced and 2 CRF6-dependent-repressed genes (Supplemental Tables S1 and S2). The magnitude of fold change of some transcripts was increased in *crf6* compared to wild type (17 [2.8%] greater induction and 3 [0.9%] greater repression; Supplemental Table S3); for such genes, loss of *CRF6* may have a more indirect effect.

Based on known DNA-binding specificity of other CRF proteins, CRF6 is predicted to interact with both GCC (AGCCGCC) and DRE ([A/G]CCGAC) motifs (Weirauch et al., 2014). In addition, CRF6 was recently shown to interact with a cytokinin responsive element in the promoter of *PIN* genes encoding auxin efflux carriers. This element was shown to contain the core G2, G5, and C7 bases shared by the GCC and DRE motifs (Šimášková et al., 2015). We examined the 2-kb upstream promoters of genes found to be differentially expressed in a CRF6-dependent manner and found that 27 of the 49 potential positive targets and 63 of the 98 potential negative targets contained at least one DRE or GCC element. Therefore, regulation of many of these genes by CRF6 could be mediated by direct transcription factor-DNA binding interactions.

Given the H_2O_2-responsive expression of *CRF6* and the H_2O_2-response phenotypes of CRF6oe, we investigated whether the constitutively elevated levels of *CRF6* in CRF6oe plants was sufficient to regulate the potential target genes we had identified. To this end, transcriptomes of untreated wild-type and CRF6oe plants were compared. Upon examination of the 49 CRF6-dependent-induced genes, we found that transcript levels of 16 of these were significantly higher in the CRF6oe background. Similarly, 41 of the 98 CRF6-dependent-represssed genes were expressed at significantly lower levels in CRF6oe (Fig. 2B; Supplemental Tables S1 and S2). Thus, for these genes, *CRF6* is necessary for a normal transcriptional response to H_2O_2 stress, and elevated levels of *CRF6*, independent of H_2O_2

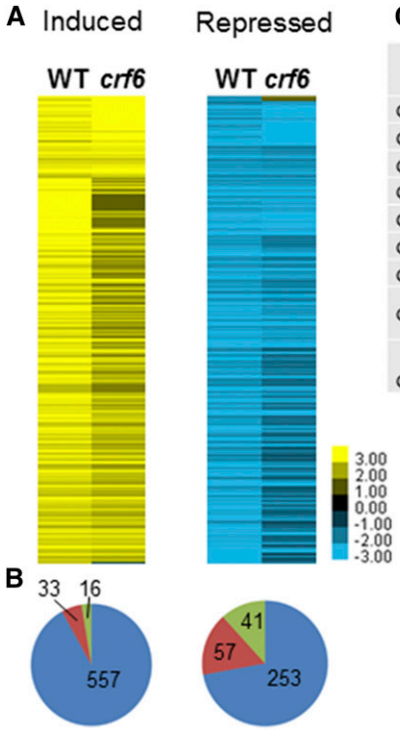

C

Term	Description	% of set	p-value	Fold Enrichment
GO:0009735	response to cytokinin stimulus	5.155	5.14E-04	13.26
GO:0009736	cytokinin mediated signaling	4.124	0.0015	17.31
GO:0015698	inorganic anion transport	4.124	0.0018	16.31
GO:0006869	lipid transport	5.155	0.0048	7.21
GO:0009664	plant-type cell wall organization	4.124	0.0057	10.88
GO:0006820	anion transport	4.124	0.0059	10.74
GO:0010876	lipid localization	5.155	0.0072	6.43
GO:0000160	two-component signal transduction system (phosphorelay)	5.155	0.0185	4.86
GO:0045338	farnesyl diphosphate metabolic process	2.062	0.0230	84.84

Figure 2. CRF6 regulation of transcriptional response to H_2O_2. A, Heat maps comparing fold change in expression of transcripts in wild-type (WT) and crf6 backgrounds after treatment with H_2O_2. The genes represented are those found to be differentially expressed in WT. B, Pie charts showing the number of transcripts in each comparison that are *CRF6* independent (blue), *CRF6* dependent (red) and *CRF6* dependent as well as similarly changed in CRF6oe vs. WT comparison (green). C, GO terms enriched among CRF6-dependent repressed genes with P value < 0.05.

Downloaded from www.plantphysiol.org on October 10, 2016 - Published by www.plantphysiol.org
Copyright © 2016 American Society of Plant Biologists. All rights reserved.

stimulus, are sufficient for a similar transcriptional response. Those genes found to be regulated in a CRF6-dependent manner, for which CRF6 overexpression was not sufficient, may require other context-specific factors for proper regulation.

CRF6 Represses Cytokinin Related Genes in Response to Oxidative Stress

To identify specific processes potentially regulated by CRF6 during oxidative stress, we examined GO terms associated with the potential CRF6 targets. When we performed an enrichment analysis of CRF6-dependent-repressed genes, the biological processes over-represented with the greatest degree of confidence were "response to cytokinin stimulus" (13.3-fold enriched, P = 5.1 E-4) and "cytokinin mediated signaling" (17.3-fold enriched, P = 1.5 E-3; Fig. 2C). Given the previously identified connections between CRF6 and cytokinin-mediated signaling/response, we chose to further examine potential targets related to these processes.

Among the CRF6-dependent-repressed genes, we identified four that encode for proteins involved in the two-component cytokinin signaling pathway (AHP1, ARR6, ARR9, and ARR11). AHP1 (ARABIDOPSIS HIS PHOSPHOTRANSFER PROTEIN 1) is involved in relaying the cytokinin signal from the membrane-bound receptors into the nucleus (Hutchison et al., 2006). ARR11 (ARABIDOPSIS RESPONSE REGULATOR 11) is 1 of 11 type-B response regulators (RR-Bs), which are GARP domain-containing MYB-related transcription factors activated within the nucleus by phosphorylation by AHPs. ARR11 is one of a subset of RR-Bs responsible for the majority of the transcriptional response to cytokinin (Hill et al., 2013). ARR6 and ARR9 are type-A response regulators, which lack DNA-binding capability and are able to compete with RR-Bs for phosphorylation to fine-tune the output of the signaling pathway (To et al., 2007). In addition to these signaling components, we identified two additional genes associated with cytokinin: LOG7 (LONELY GUY 7) and ABCG14 (ATP-BINDING CASSETTE G14). LOG7 catalyzes a key step in the synthesis of the active form of cytokinin, and ABCG14 is a transporter essential for long-distance translocation of cytokinin (Tokunaga et al., 2012; Ko et al., 2014). Together, these six genes are necessary components of three major aspects of cytokinin function in plants: signaling, biosynthesis, and transport.

We examined the expression of these potential targets in the transcriptomes of untreated CRF6oe and wild-type plants to determine whether constitutive overexpression of *CRF6* is sufficient to repress these target genes. Strikingly, all but one (AHP1) were also expressed at lower basal levels in CRF6oe plants than in wild type (Fig. 3A). To confirm the regulation of these genes by CRF6 (as well as the transcriptome analysis in general), we examined expression patterns using qRT-PCR. The five cytokinin-related targets examined were found to be repressed by H_2O_2 stress in wild-type plants; this repression was absent or attenuated in *crf6* mutants (Supplemental Fig. S2). Reduced expression in CRF6oe plants was also supported by qRT-PCR (Fig. 3B).

To determine whether CRF6 might repress these genes through direct promoter-binding interactions, we carried out a targeted yeast one-hybrid screen. Promoter segments from within 2 kb upstream of ATG, containing any GCC-motifs and/or degenerate versions thereof, were used as baits for the full-length CRF6 coding sequence fused to the GAL4 activation domain as prey. The only high-confidence interaction detected was between *CRF6* and the promoter of *ARR6* (Fig. 3C; Supplementary Figs. S3 and S4). Interestingly, ARR6 was also the only promoter sequence tested that contained a true, nondegenerate GCC-motif (AGCCGCC). A recent study using a root protoplast-based luciferase activation assay demonstrated that CRF6 regulates the expression of auxin transporters (PINs) in Arabidopsis roots. This regulation was shown to occur through interactions of CRF6 with upstream enhancer elements containing the motif AG[A/C]AGAC, which has the conserved G2, G5, and C7 bases (underlined) that are essential for interaction with AP2/ERF family transcription factors (Šimášková et al., 2015). As similar motifs are present in the promoters of each of the cytokinin-related targets, we employed the same assay here to determine whether CRF6 could activate these promoters within the context of a plant cell. In this assay, CRF6 was again found to activate with the ARR6 promoter similar to the Y1H direct binding (Fig. 3D). We also found CRF6 interactions with the promoters of ARR9 and LOG7 not found in Y1H, suggesting that additional plant-specific factors are required for these interactions. Different from Y1H, the protoplast-luciferase-activation assay has been shown to be capable of differentiating between inductive and repressive regulation. Although our prior results indicate that CRF6 acts to repress these genes, expression was shown as induced in this system. This unexpected result may again reflect the context-specific nature of CRF6 repression during oxidative stress. For example, stress-induced posttranslational modifications or additional transcription factors not expressed in root protoplasts may be required for proper regulation. Despite this ambiguity, these data indicate that CRF6 regulates the expression of ARR6 (and possibly others) through direct interaction with its promoter.

To gain further insight into and support for the role of the cytokinin-associated genes downstream of CRF6 in oxidative stress response, we examined whether mutants of these target genes have altered oxidative stress response phenotypes. We obtained T-DNA insertional mutants of the five cytokinin-associated genes with reduced basal expression in CRF6oe plants (*arr6*, *arr9*, *arr11*, *abcg14*, and *log7*; To et al., 2007; Ko et al., 2014; Alonso et al., 2003). Both whole seedlings and leaves from these mutants, along with the lines used for transcriptome analyses (CRF6oe19.3, *crf6-2*, and Col-0) and an additional, previously described line overexpressing

Downloaded from www.plantphysiol.org on October 10, 2016 - Published by www.plantphysiol.org
Copyright © 2016 American Society of Plant Biologists. All rights reserved.

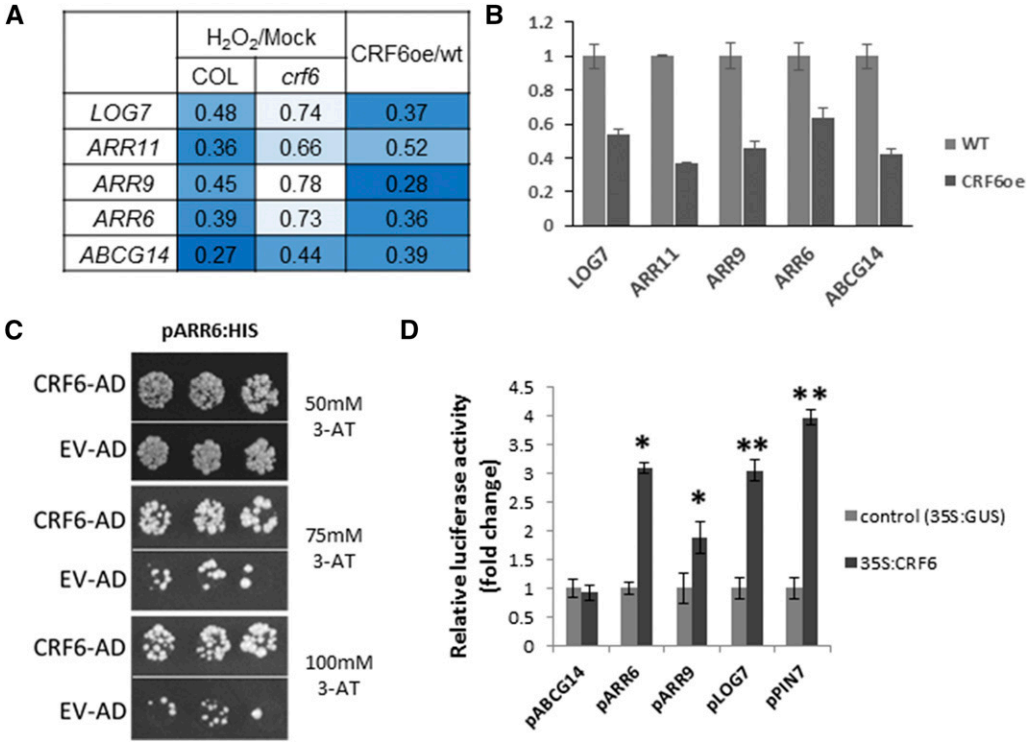

Figure 3. CRF6 regulates the expression of a subset of cytokinin-related genes in response to H_2O_2. A, Ratios of normalized expression values determined by microarray analysis of cytokinin-related genes. For each gene, the ratio of expression H_2O_2/mock in the wild-type (WT) and *crf6* backgrounds is given along with the ratio CRF6oe/WT ratio. B, Graph of ratio of expression CRF6oe/WT determined by qRT-PCR. C, Yeast one-hybrid assay of CRF6 interaction with the upstream promoter sequence of ARR6. Shown are three independent transformations of CRF6-AD or Empty AD Vector (EV-AD) plated on media containing the indicated concentrations of 3-AT. D, Fold change in relative luciferase activity of indicated promoters coexpressed with 35S:CRF6 as compared to 35S:GUS controls.

CRF6 (CRF6ox3 from Zwack et al., 2013), were treated with H_2O_2 (20 mM) or AA (5 mM) for 48 h. As previously observed, *CRF6*-overexpressing plants demonstrated significantly less reduction in Fv/Fm after H_2O_2 treatment of both seedlings and detached leaves compared to mock-treated controls. We observed a similar stress-related phenotype for all five target gene mutants (*arr6*, *arr9*, *arr11*, *log7*, and *abcg14*; Fig. 4, A and B). To further examine these lines after oxidative stress along with Fv/Fm measurements, Rfd the fluorescence decline ratio was measured in leaves (Lichtenthaler and Miehé, 1997; Zhang et al., 2016). Results of Rfd levels after oxidative stress H_2O_2 (20 mM) and AA (5 mM) treatments (Fig. 4, C and D) parallel the Fv/Fm findings after H_2O_2 (Fig. 4, A and B). CRF6oe lines had significantly less reduction in Rfd than wild type, while *crf6-2* had a significantly greater reduction and target gene mutants were generally affected in a manner similar to the CRF6oe lines. In addition to these changes in photosynthetic efficiency, CRF6oe and cytokinin mutant leaves also displayed less visible discoloration than wild type after oxidative stress exposure (Fig. 4E). Finally, chlorophyll levels were determined in leaves of these same lines in the presence and absence of H_2O_2 (20 mM). The reduction in chlorophyll levels, shown as a percent of untreated levels, again paralleled both Fv/Fm and Rfd measurements (Fig. 4F; Supplementary Fig. S5). Overall, these stress-related phenotypic similarities to CRF6oe lines support these five genes as targets of repression functionally downstream of CRF6. Importantly, this repression also seems to be necessary for wild-type response to stress under these conditions, as *crf6* mutants (in which the down-regulation of these genes does not occur) shows significantly decreased oxidative stress response in both whole seedlings and detached leaves (Fig. 4). Collectively, the results presented in this study demonstrate a mechanistic link between cytokinin and oxidative stress: a set of cytokinin associated genes are repressed downstream of *CRF6* in response to H_2O_2 and the resulting low levels of expression modulate the response to oxidative stress.

DISCUSSION

Plant responses to oxidative stress provoking conditions are crucial for survival. As such, these responses are highly regulated and must be specific to conditions both external, such as the environment, as well as internal, such as developmental status. This regulation can be achieved through cross-talk between various signaling pathways, including several plant hormones

Downloaded from www.plantphysiol.org on October 10, 2016 - Published by www.plantphysiol.org
Copyright © 2016 American Society of Plant Biologists. All rights reserved.

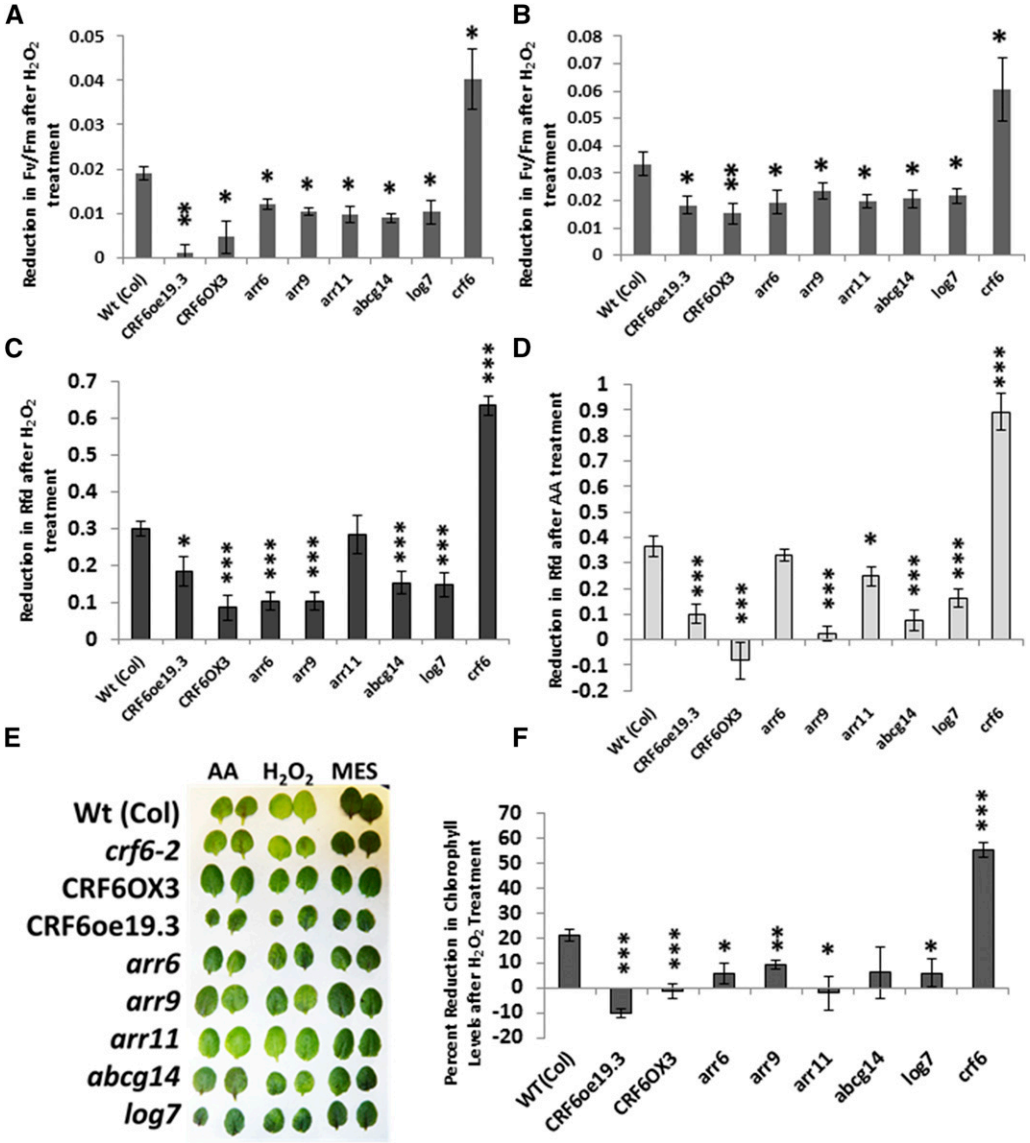

Figure 4. Effects of oxidative stress on cytokinin-related targets of CRF6. A and B, Reduction in Fv/Fm of leaves from H_2O_2 treatment of 5-d-old whole seedlings (A) and detached leaves 5/6 from 17-d-old plants (B). C and D, Reduction in Rfd from H_2O_2 (C) or AA (D) treatment of detached leaves 3/4 from 14-d-old plants (E) Appearance of leaves after incubation with AA, H_2O_2, or MES buffer alone. F, Percent reduction in chlorophyll levels (measured as nmol/mg fresh weight) after H_2O_2 treatment of detached leaves 3/4 from 14-d-old plants. Genotypes are as indicated. Treatments were made with 20 mM H_2O_2 or 5 mM AA for 48 h. Significant difference compared to wild type (WT) indicated by $*P < 0.05$, $**P < 0.01$, $***P < 0.001$ (Student's *t*-test).

known to have a role in the regulation of stress responses; such a role for cytokinin has recently gained support (O'Brien and Benková, 2013; Argueso et al., 2009; Ha et al., 2012; Zwack and Rashotte, 2015). Expression of the Arabidopsis transcription factor CRF6 is induced by both cytokinin and oxidative stress, indicating a possible connection between these pathways (Zwack et al., 2013; De Clercq et al., 2013; Ng et al., 2013). In response to cytokinin, *CRF6* has been shown to play a role in the inhibition of leaf senescence; however, the functional relevance of its induction by oxidative stress was unknown. Interestingly, transcriptional induction of *CRF6* in response to stress appears to be independent of cytokinin; a comparison of transcriptional changes as a result of salt stress in wild-type and cytokinin-deficient mutant Arabidopsis plants showed that expression of *CRF6* was up-regulated in both backgrounds (Nishiyama et al., 2012). Here, we demonstrated that expression of *CRF6* partially mediates responses to H_2O_2 and that plants constitutively overexpressing *CRF6* are able to maintain both photosynthetic efficiency and root growth better than wild-type plants when exposed to oxidative stress-inducing conditions (Fig. 1).

Downloaded from www.plantphysiol.org on October 10, 2016 - Published by www.plantphysiol.org
Copyright © 2016 American Society of Plant Biologists. All rights reserved.

To examine the mechanism by which this transcription factor regulates response to oxidative stress, we analyzed genome-wide differences in transcriptional response to H_2O_2 of *crf6* knockout mutants and wild-type plants. From this analysis, genes requiring CRF6 for their responsiveness to H_2O_2, or CRF6-dependent genes, were identified. A much greater proportion of CRF6-dependent genes was repressed (28%) than induced (8%) in wild type in response to H_2O_2 stress, suggesting that CRF6 functions largely as a transcriptional repressor under these conditions (Fig. 2B; Supplemental Tables S1 and S2). Interestingly, we identified a set of six genes involved in various fundamental aspects cytokinin function (biosynthesis, transport, and signal transduction) that are repressed downstream of CRF6 during oxidative stress. We further investigated these genes as a potential functional module of cytokinin-associated genes that is repressed during oxidative stress (Fig. 3). We demonstrated oxidative stress response phenotypes for the *arr6*, *arr9*, *arr11*, *log7*, and *abcg14* loss-of-function mutants that are similar to plants overexpressing *CRF6*. In addition, we found *crf6* loss-of-function plants have the opposite oxidative-stress-response phenotype to the overexpression lines. Together, this strongly supports these genes as being repressed by CRF6 in response to oxidative stress and the notion that this repression is part of the mechanism by which oxidative stress response is altered in CRF6oe plants (Fig. 4). More detailed analyses of CRF6-target-promoter interactions indicated regulation by CRF6 may be indirect for most genes in the module (Fig. 3). Nonetheless, our transcriptional analyses in conjunction with the mutant phenotype results clearly indicate that CRF6 is involved in the oxidative stress-triggered repression of these genes. Importantly, we identified an interaction between CRF6 and the promoter of ARR6, suggesting that CRF6 may act to directly regulate some of its targets (Fig. 3, C and D).

Our findings provide strong evidence that CRF6 mediates a crucial interaction between oxidative stress responses and cytokinin. Cytokinin is involved in a wide range of indispensable processes throughout the plant, yet it is known to have a negative impact on stress tolerance (O'Brien and Benková, 2013; Argueso et al., 2009; Ha et al., 2012; Zwack and Rashotte, 2015). Additionally, increased cytokinin levels have been shown to increase endogenous ROS production (Wang et al., 2015). If and by what means a plant could overcome the antagonistic effects of cytokinin has until now remained unclear. Our results provide a clear mechanism by which this effect can occur: in response to oxidative stress, CRF6 down-regulates the expression of genes involved in various aspects of the biological function of cytokinin (biosynthesis, transport, and signaling), possibly allowing for improved stress response. Here, we have used oxidative stress to demonstrate this mechanism, but we speculate that a similar response to other stresses may also occur, as a wide range of stress conditions can lead to both ROS production and increased expression of CRF6.

MATERIALS AND METHODS

Plant Material and Growth Conditions

All transgenic lines were generated in the Col-0 background. Both CRF6ox3 and *crf6*$^{-2}$ (Zwack et al., 2013) and CRF6oe19.3 and 19.7 (Inzé et al., 2012) were previously described. The CRF6 overexpression line 19.3 was kindly provided by Frank Hoeberichts. T-DNA insertional mutants *arr6*, *arr9*, *arr11-3* (SALK_006544), *log7* (SALK_113173C), and *abcg14* (SK_15918) were obtained from the Arabidopsis Biological Resources Center. Unless otherwise stated, plants were sterilized and sown on plates containing full-strength Murashige and Skoog (MS) medium and 1% Suc buffered with MES at pH 5.7. After 2 d at 4°C, plates were moved to a controlled environmental chamber and grown under diurnal conditions of 16 h light (100 μE) at 22°C and 8 h dark at 18°C. For root growth, seedlings were transferred at day 4 to new plates either as described above (MS) or supplemented with 5 mM AA and allowed to grow until day 9 when the day 4 to 9 growth was measured as previously described (Rashotte et al., 2006). Root growth was measured in three independent experiments with 10 or more samples per replicate (±) per treatment. For extended growth (>10 d after germination), plants were moved to soil (sunshine mix no. 8) and grown under similar conditions but at approximately 150 μE light.

Chlorophyll Fluorescence Analyses

Treatments with H_2O_2, AA, or 3-AT were carried out on either whole seedlings (3 d old) or from leaves 3/4 or 5/6 excised from 14- to 20-d-old plants as noted in the text. Leaves were cut and immediately floated abaxial side down on deionized water buffered with 3 mM MES (pH 5.7). Cut leaves were dark-adapted for 30 min before initial chlorophyll fluorescence was measured using standard setting from FluroCam7 software on a Handy FluorCam, Photon Systems Instruments: $F_v/F_m = (F_m\text{-}F_o)/F_m$ as maximum PSII quantum efficiency or Rfd = $(F_P - Ft\_Lss) / FP$), the fluorescence decline ratio using peak fluorescence (F_P) and steady-state fluorescence in the terminal light-adapted phase (*Ft_Lss*). Leaves were then transferred to individual wells of 6- to 24-well plates containing a similarly buffered solution of either 20 mM H_2O_2, 5 mM AA, or 10 mM 3-AT. The plates were covered (not sealed) and returned to the growth chamber under normal conditions. After 24 to 48 h, leaves were again dark-adapted and chlorophyll fluorescence was measured. For chlorophyll measurements, cut leaves treated as above were weighed, then placed in methanol 4C overnight and examined using a spectrophotometer to yield chlorophyll levels (nmol/mg fresh weight) as previously described (Zwack et al., 2013). All experiments were performed three to six times with three to ten samples per replicate (±) for each treatment.

For the photorespiratory-promoting conditions, plants were grown on MS medium for 2 weeks at 21°C and 100 μE light intensity in a 16-h-light/8-h-dark photoperiod. Then, plates were sealed with two layers of parafilm M (Bemis) to restrict the gas exchange (RG) and grown as above. Following 30 min dark adaptation, dark fluorescent parameters (F_o, F_m) were determined using a PAM-2000 chlorophyll fluorometer and ImagingWin software application (Walz). Then, after an additional 40 s of darkness, light-induced changes in fluorescence parameters (F and F_m') were monitored every 20 s under (normal) actinic light 186 μE for 5 min. The minimum fluorescence yield of the illuminated sample (F_0') was estimated from F_m' values using $F_0' = F_0/[(F_v/F_m)+(F_0/F_m')]$. Maximum PSII quantum efficiency is determined by $F_v/F_m = (F_m\text{-}F_o)/F_m$; the effective PSII quantum efficiency, $\Phi II = (F_m'\text{-}F)/F_m'$; the PSII efficiency factor (estimation of the fraction of reaction centers in the open state), $qP = (F_m'\text{-}F)/(F_m'\text{-}F_0')$; $NPQ = (F_m\text{-}F_m')/F_m'$.

Expression Analyses

Ten-day-old plants were removed from plates and floated on 3 mM MES buffer pH 5.7. After 1 h treatment, sample had H_2O_2 added to a final concentration of 20 mM. Treatment and control solutions both contained 0.2% dimethyl sulfoxide. Plants were treated for 6 h then immediately frozen in liquid nitrogen. For each treatment, approximately 10 individual plants were pooled for analysis.

RNA from two independent experiments was isolated using the Qiagen RNeasy Plant Mini-kit according to the manufacturer's instructions. Hybridization to Affymetrix Arabidopsis Gene 1.0 ST arrays, scanning, and raw data preprocessing were performed as a service by the Heflin Center for Genomic Science at the University of Alabama-Birmingham.

Normalization and differential expression analyses were performed using the FlexArray 1.6 software package from McGill University and Genome Quebec. Normalization was performed using algorithms provided by Affymetrix. Fold change in expression was calculated by Cyber-T analysis, and

Downloaded from www.plantphysiol.org on October 10, 2016 - Published by www.plantphysiol.org
Copyright © 2016 American Society of Plant Biologists. All rights reserved.

adjusted *P* values were determined using the Benjamini Hochberg method of False Discovery Rate.

qRT-PCR verification was carried out using Sybr-Green and sequence specific primers. Reactions were carried out as previously described (Zwack et al., 2013).

Yeast One-Hybrid

The enhanced yeast one-hybrid assay was performed as previously reported (Gaudinier et al., 2011). Briefly, the promoters of *ABCG14*, *AHP1*, *ARR6*, *ARR9*, *ARR11*, and *LOG7* were amplified via PCR (5x Phire reaction buffer, 0.25 μM of each of the primers, 0.2 mM dNTPs, Phire Hot Start II DNA Polymerase [Thermo Scientific], and Arabidopsis genomic DNA) using primers designed to introduce the Gateway *att*P4 and *att*P1 cassette sequences. The initial denaturation step occurred at 94°C for 5 min followed by 40 cycles of 18 s at 94°C, 30 s at 58°C, and 1 min at 72°C. The final elongation step was 7 min at 72°C. The PCR products were transferred into the pDONR P4-P1R vector (Invitrogen) using Gateway BP recombination (2 μL 5x BP Clonase II enzyme mix, 150 ng PCR product, 150 ng empty P4-P1R vector). P4-P1R promoter Entry clones were transferred into the pMW#2 vector containing the reporter gene *HIS3* by Gateway LR recombination (1 μL 5× LR Clonase II enzyme mix, 150 ng P4-P1R Entry clone, and 150 ng empty pMW2 vector). Additionally, *CRF6* was transferred to a pDEST-AD vector by LR cloning to create a CRF6-Gal4 activating domain fusion protein.

The promoter:*HIS3* sequences were integrated into the genome of the haploid yeast (*Saccharomyces cerevisiae*) strain YM4271, and the pDEST-AD-CRF6 was transformed into the strain Yα1867 as previously described to create the bait and preys, respectively (Deplancke et al., 2006; Reece-Hoyes et al., 2011). The transformed haploid baits were grown on minimum selective media containing all necessary amino acids except His (synthetic dropout [SD-HT]), and the transformed haploid preys were selected on SD-T (Trp). The haploid baits and preys were mated pairwise overnight in liquid yeast extract peptone dextrose. The resulting diploid yeast cells were grown overnight in liquid SD-HT. The diploid yeast cells were plated on solid SD-HT media containing varying concentrations (from 0 to 100 mM) of 3-AT. The pDEST-AD vector was also transformed into Yα1867 and mated with each bait to serve as a negative control.

Transient Expression in Root Suspension Culture Protoplasts

The luciferase assays were performed on 4-d-old Arabidopsis (*Arabidopsis thaliana*) root suspension culture by PEG-mediated transformation. Protoplasts were isolated in enzyme solution (1% cellulose; Serva, 0.2% Macerozyme; Yakult in B5-0.34M Glc-mannitol solution; 2.2 g MS with vitamins, 15.25 g Glc, 15.25 g mannitol, H_2O to 500 mL, pH to 5.5, with KOH) with slight shaking for 3 to 4 h, centrifuged at 800 g for 5 min. The pellet was washed with B5-0.34M Glc-mannitol solution and resuspended in B5-0.34M Glc-mannitol solution to a final concentration of 2×10^5 protoplasts per 50 μL. Protoplasts were cotransfected with 1 μg of a reporter plasmid that contained *Firefly* luciferase (*f*LUC), 1 μg of effector construct, and 2 μg of normalization plasmid expressing the *Renilla* luciferase (*r*LUC) under the control of the 35S promoter. The total amount of DNA was equalized in each experiment with the *p2GW7-GUS* mock effector plasmid. DNAs were gently mixed together with 50 μL of protoplast suspension and 60 μL of PEG solution [0.1M $Ca(NO_3)_2$, 0.45M mannitol, 25% PEG 6000] and incubated in the dark for 30 min. Then 140 μL of 0.275M $Ca(NO_3)_2$ solution was added to wash off PEG and waited for sedimentation of protoplasts and removed 240 μL of supernatant. The protoplast pellet was resuspended in 200 μL ofB5-0.34M Glc-mannitol solution and incubated for 16 h in the dark at room temperature. After transfection, protoplasts were centrifuged at 1200 g for 5 min and analyzed; *f*LUC and *r*LUC activities were determined with the Dual-Luciferase reporter assay system (Promega). Variations in transfection efficiency and technical errors were corrected by normalization of *f*LUC by the *r*LUC activities. The mean value was calculated from six measurements and experiment was repeated two times.

Accession Numbers

Sequence data from this article can be found in the GenBank/EMBL data libraries under accession numbers GSE84770.

Supplemental Data

The following supplemental materials are available.

Supplemental Figure S1. Chlorophyll fluorescence responses to photorespiratory-inducing conditions of plants overexpressing CRF6.

Supplemental Figure S2. Graph of ratio of expression H2O2/mock in the wild-type and crf6 backgrounds as determined by qRT-PCR.

Supplemental Figure S3. Schematic representation of promoter sequences used in luciferase transactivation and yeast one-hybrid assays.

Supplemental Figure S4. Results of yeast one-hybrid screen.

Supplemental Figure S5. Effects of oxidative stress on chlorophyll levels of cytokinin-related targets of CRF6.

Supplemental Table S1. Expression of CRF6-dependent-induced genes.

Supplemental Table S2. Expression of CRF6-dependent-repressed genes.

Supplemental Table S3. Expression of genes showing enhanced regulation in the absence of CRF6.

ACKNOWLEDGMENTS

We thank Michael Crowley, Ph.D. at the Heflin Center for Genomic Science at UAB and Sophia Zebell for critical reading of the manuscript.

Received May 11, 2016; accepted August 18, 2016; published August 22, 2016.

LITERATURE CITED

Alonso JM, Stepanova AN, Leisse TJ, Kim CJ, Chen H, Shinn P, Stevenson DK, Zimmerman J, Barajas P, Cheuk R, et al (2003) Genome-wide insertional mutagenesis of Arabidopsis thaliana. Science **301:** 653–657

Argueso CT, Ferreira FJ, Kieber JJ (2009) Environmental perception avenues: the interaction of cytokinin and environmental response pathways. Plant Cell Environ **32:** 1147–1160

Baker NR (2008) Chlorophyll fluorescence: a probe of photosynthesis in vivo. Annu Rev Plant Biol **59:** 89–113

Cutcliffe JW, Hellmann E, Heyl A, Rashotte AM (2011) CRFs form protein-protein interactions with each other and with members of the cytokinin signalling pathway in Arabidopsis via the CRF domain. J Exp Bot **62:** 4995–5002

De Clercq I, Vermeirssen V, Van Aken O, Vandepoele K, Murcha MW, Law SR, Inzé A, Ng S, Ivanova A, Rombaut D, et al (2013) The membrane-bound NAC transcription factor ANAC013 functions in mitochondrial retrograde regulation of the oxidative stress response in Arabidopsis. Plant Cell **25:** 3472–3490

Deplancke B, Vermeirssen V, Arda HE, Martinez NJ, Walhout AJ (2006) Gateway-compatible yeast one-hybrid screens. CSH Protoc **2006:** doi/10.1101/pdb.prot4590

Gaudinier A, Zhang L, Reece-Hoyes JS, Taylor-Teeples M, Pu L, Liu Z, Breton G, Pruneda-Paz JL, Kim D, Kay SA, et al (2011) Enhanced Y1H assays for Arabidopsis. Nat Methods **8:** 1053–1055

Genty B, Briantais J-M, Baker NR (1989) The relationship between the quantum yield of photosynthetic electron transport and quenching of chlorophyll fluorescence. Biochim Biophys Acta **990:** 87–92

Gill SS, Tuteja N (2010) Reactive oxygen species and antioxidant machinery in abiotic stress tolerance in crop plants. Plant Physiol Biochem **48:** 909–930

Ha S, Vankova R, Yamaguchi-Shinozaki K, Shinozaki K, Tran LSP (2012) Cytokinins: metabolism and function in plant adaptation to environmental stresses. Trends Plant Sci **17:** 172–179

Hill K, Mathews DE, Kim HJ, Street IH, Wildes SL, Chiang YH, Mason MG, Alonso JM, Ecker JR, Kieber JJ, et al (2013) Functional characterization of type-B response regulators in the Arabidopsis cytokinin response. Plant Physiol **162:** 212–224

Hutchison CE, Li J, Argueso C, Gonzalez M, Lee E, Lewis MW, Maxwell BB, Perdue TD, Schaller GE, Alonso JM, et al (2006) The Arabidopsis histidine phosphotransfer proteins are redundant positive regulators of cytokinin signaling. Plant Cell **18:** 3073–3087

Inzé A, Vanderauwera S, Hoeberichts FA, Vandorpe M, Van Gaever T, Van Breusegem F (2012) A subcellular localization compendium of hydrogen peroxide-induced proteins. Plant Cell Environ **35:** 308–320

Jeon J, Kim NY, Kim S, Kang NY, Novák O, Ku SJ, Cho C, Lee DJ, Lee EJ, Strnad M, et al (2010) A subset of cytokinin two-component signaling system plays a role in cold temperature stress response in Arabidopsis. J Biol Chem **285:** 23371–23386

Downloaded from www.plantphysiol.org on October 10, 2016 - Published by www.plantphysiol.org
Copyright © 2016 American Society of Plant Biologists. All rights reserved.

Ko D, Kang J, Kiba T, Park J, Kojima M, Do J, Kim KY, Kwon M, Endler A, Song W-Y, et al (2014) Arabidopsis ABCG14 is essential for the root-to-shoot translocation of cytokinin. Proc Natl Acad Sci USA **111:** 7150–7155

Lichtenthaler HK, Miehé JA (1997) Fluorescence imaging as a diagnostic tool for plant stress. Trends Plant Sci **2:** 316–320

Macková H, Hronková M, Dobrá J, Turečková V, Novák O, Lubovská Z, Motyka V, Haisel D, Hájek T, Prášil IT, et al (2013) Enhanced drought and heat stress tolerance of tobacco plants with ectopically enhanced cytokinin oxidase/dehydrogenase gene expression. J Exp Bot **64:** 2805–2815

Mason MG, Jha D, Salt DE, Tester M, Hill K, Kieber JJ, Schaller GE (2010) Type-B response regulators ARR1 and ARR12 regulate expression of AtHKT1;1 and accumulation of sodium in Arabidopsis shoots. Plant J **64:** 753–763

Mittler R (2002) Oxidative stress, antioxidants and stress tolerance. Trends Plant Sci **7:** 405–410

Ng S, Ivanova A, Duncan O, Law SR, Van Aken O, De Clercq I, Wang Y, Carrie C, Xu L, Kmiec B, et al (2013) A membrane-bound NAC transcription factor, ANAC017, mediates mitochondrial retrograde signaling in Arabidopsis. Plant Cell **25:** 3450–3471

Nishiyama R, Le DT, Watanabe Y, Matsui A, Tanaka M, Seki M, Yamaguchi-Shinozaki K, Shinozaki K, Tran LSP (2012) Transcriptome analyses of a salt-tolerant cytokinin-deficient mutant reveal differential regulation of salt stress response by cytokinin deficiency. PLoS One **7:** e32124

Nishiyama R, Watanabe Y, Fujita Y, Le DT, Kojima M, Werner T, Vankova R, Yamaguchi-Shinozaki K, Shinozaki K, Kakimoto T, et al (2011) Analysis of cytokinin mutants and regulation of cytokinin metabolic genes reveals important regulatory roles of cytokinins in drought, salt and abscisic acid responses, and abscisic acid biosynthesis. Plant Cell **23:** 2169–2183

Nguyen KH, Ha CV, Nishiyama R, Watanabe Y, Leyva-González MA, Fujita Y, Tran UT, Li W, Tanaka M, Seki M et al (2016) Arabidopsis type B cytokinin response regulators ARR1, ARR10, and ARR12 negatively regulate plant responses to drought. Proc Natl Acad Sci USA **113:** 3090–3095

O'Brien JA, Benková E (2013) Cytokinin cross-talking during biotic and abiotic stress responses. Front Plant Sci **4:** 451

Petrov VD, Van Breusegem F (2012) Hydrogen peroxide-a central hub for information flow in plant cells. AoB Plants **2012:** pls014

Rashotte AM, Mason MG, Hutchison CE, Ferreira FJ, Schaller GE, Kieber JJ (2006) A subset of Arabidopsis AP2 transcription factors mediates cytokinin responses in concert with a two-component pathway. Proc Natl Acad Sci USA **103:** 11081–11085

Reece-Hoyes JS, Diallo A, Lajoie B, Kent A, Shrestha S, Kadreppa S, Pesyna C, Dekker J, Myers CL, Walhout AJ (2011) Enhanced yeast one-hybrid assays for high-throughput gene-centered regulatory network mapping. Nat Methods **8:** 1059–1064

Šimášková M, O'Brien JA, Khan M, Van Noorden G, Ötvös K, Vieten A, De Clercq I, Van Haperen JM, Cuesta C, Hoyerová K, et al (2015) Cytokinin response factors regulate PIN-FORMED auxin transporters. Nat Commun **6:** 8717–8727

Suzuki N, Koussevitzky S, Mittler R, Miller G (2012) ROS and redox signalling in the response of plants to abiotic stress. Plant Cell Environ **35:** 259–270

To JPC, Deruère J, Maxwell BB, Morris VF, Hutchison CE, Ferreira FJ, Schaller GE, Kieber JJ (2007) Cytokinin regulates type-A Arabidopsis Response Regulator activity and protein stability via two-component phosphorelay. Plant Cell **19:** 3901–3914

Tokunaga H, Kojima M, Kuroha T, Ishida T, Sugimoto K, Kiba T, Sakakibara H (2012) Arabidopsis lonely guy (LOG) multiple mutants reveal a central role of the LOG-dependent pathway in cytokinin activation. Plant J **69:** 355–365

Tran L-SP, Urao T, Qin F, Maruyama K, Kakimoto T, Shinozaki K, Yamaguchi-Shinozaki K (2007) Functional analysis of AHK1/ATHK1 and cytokinin receptor histidine kinases in response to abscisic acid, drought, and salt stress in Arabidopsis. Proc Natl Acad Sci USA **104:** 20623–20628

Wang Y, Shen W, Chan Z, Wu Y (2015) Endogenous cytokinin overproduction modulates ROS homeostasis and decreases salt stress resistance in *Arabidopsis thaliana*. Front Plant Sci **6:** 1004

Weirauch MT, Yang A, Albu M, Cote AG, Montenegro-Montero A, Drewe P, Najafabadi HS, Lambert SA, Mann I, Cook K, et al (2014) Determination and inference of eukaryotic transcription factor sequence specificity. Cell **158:** 1431–1443

Wrzaczek M, Brosché M, Kangasjärvi J (2013) ROS signaling loops - production, perception, regulation. Curr Opin Plant Biol **16:** 575–582

Zhang L, Kondo H, Kamikubo H, Kataoka M, Sakamoto W (2016) VIPP1 has a disordered C-terminal tail necessary for protecting photosynthetic membranes against stress in Arabidopsis. Plant Physiol **171:** 1983–1995

Zwack PJ, Rashotte AM (2015) Interactions between cytokinin signalling and abiotic stress responses. J Exp Bot **66:** 4863–4871

Zwack PJ, Robinson BR, Risley MG, Rashotte AM (2013) Cytokinin response factor 6 negatively regulates leaf senescence and is induced in response to cytokinin and numerous abiotic stresses. Plant Cell Physiol **54:** 971–981

Downloaded from www.plantphysiol.org on October 10, 2016 - Published by www.plantphysiol.org
Copyright © 2016 American Society of Plant Biologists. All rights reserved.

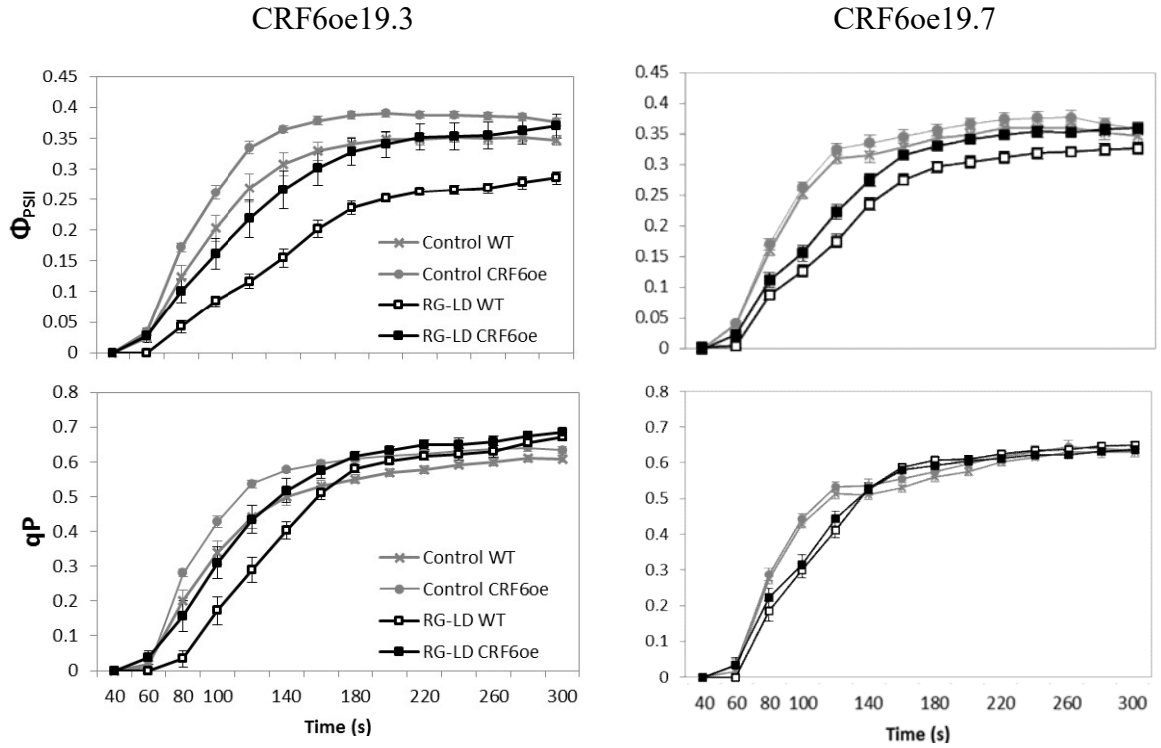

Supplemental Fig.1 Chlorophyll fluorescence responses to photorespiratory-inducing conditions of plants overexpressing *CRF6* . Additional parameter calculated from data used in **Fig. 1 d&e**. See results and methods in main text for details.

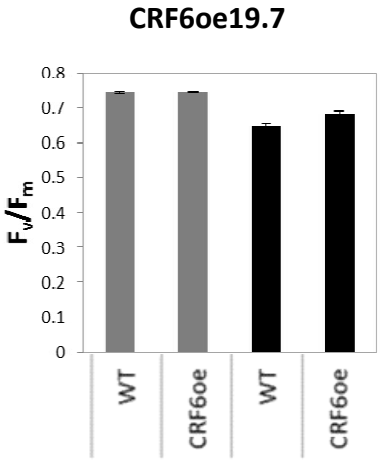

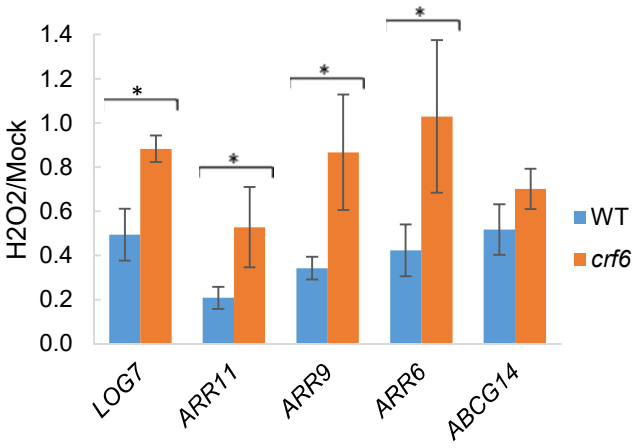

Supplemental Fig.2 Graph of ratio of expression H_2O_2/Mock in the WT and *crf6* backgrounds as determined by qRT-PCR.

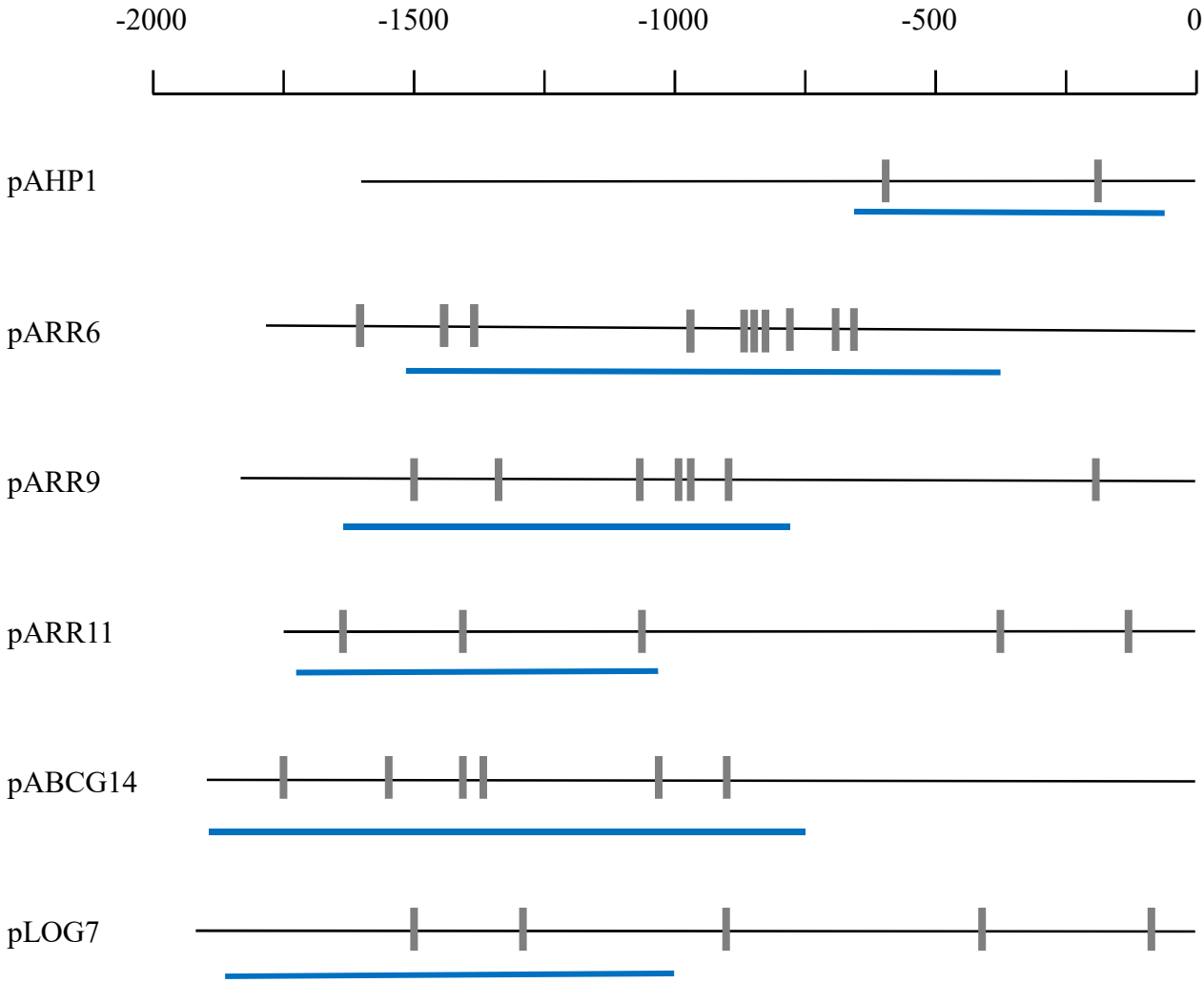

Supplemental Fig. 3. Schematic representation of promoter sequences used in Luciferase transactivation and Yeast 1-hybrid assays. Black lines represent sequence upstream of translational start site (0), Grey bars indicate approximate position of NGNNGNC motifs. For Luciferase transactivation, the full sequence lengths shown were used. For Y1-h, the fragments underlined in blue were used.

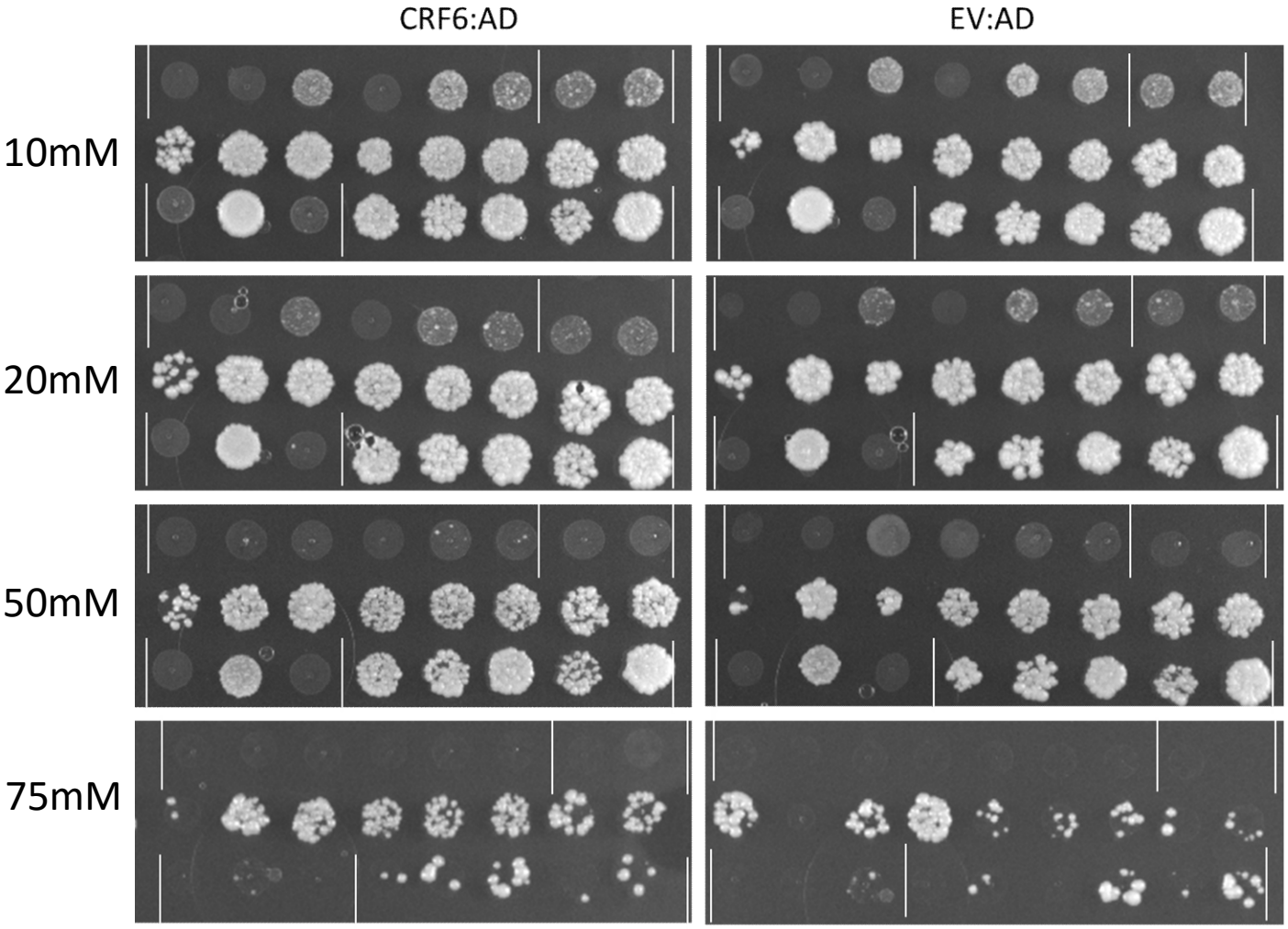

pARR11	pARR9
pARR6	
pAHP1	pABCG14

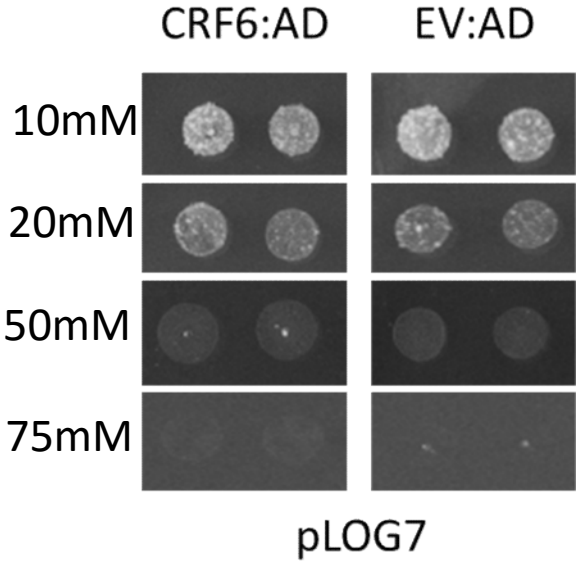

Supplemental Fig.4 Results of Yeast 1-hybrid screen. Diploid yeast resulting from mating strains carrying the indicated AD and promoter constructs grown on selective media containing indicated concentrations of 3-AT. Each colony represents an independent transformation of the promoter construct. See materials and methods for details.

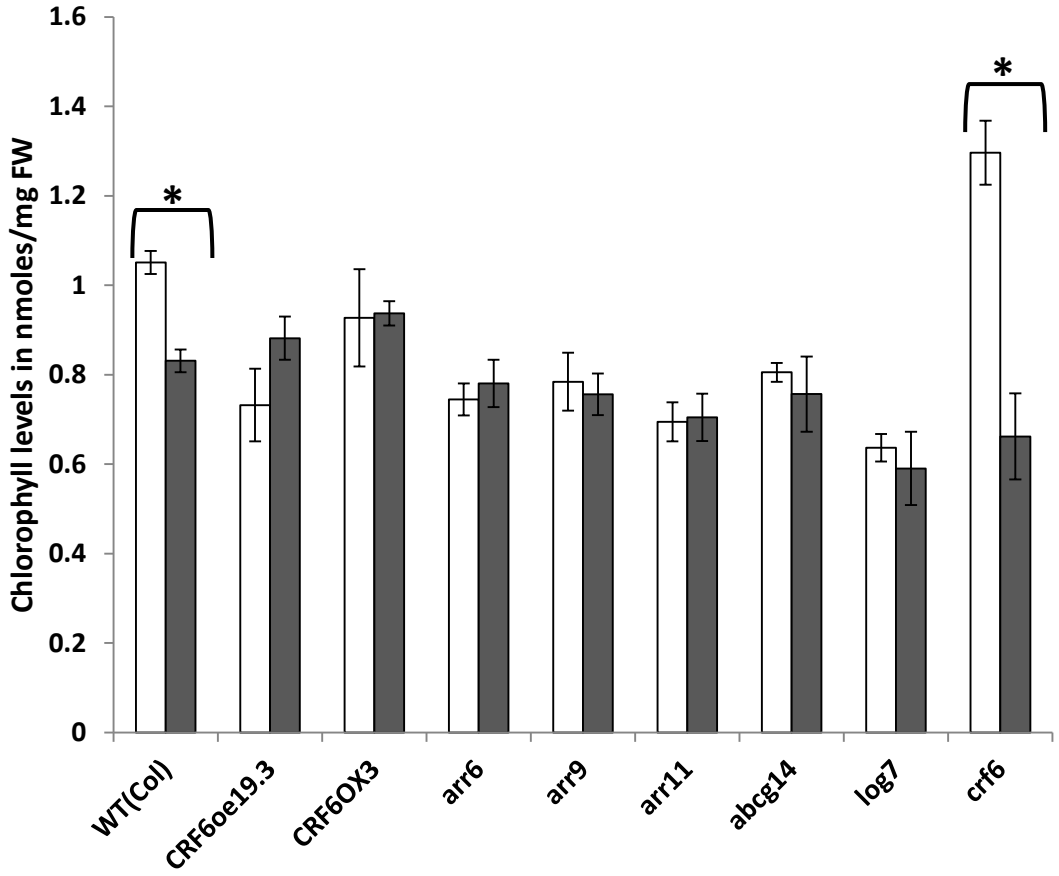

Supplemental Fig. 5. Effects of Oxidative stress on chlorophyll levels of cytokinin-related targets of CRF6. Chlorophyll levels as measured in nmoles/mg FW after 48h treatment with 20mM H_2O_2 of detached leaves 3/4 from 14d old plants, as seen in Fig. 4. Genotypes are as indicated. White bar indicates MES treated control. Gray bar indicates H_2O_2 treatment. Significant difference compared between a treated and untreated genotype indicated by *, $p < 0.05$ (Student's T-Test).

Supplemental Information Appendix

Supplementary Table 1. Expression of CRF6-dependent-induced genes

Locus ID	Gene Symbol	Col-0 H_2O_2/Mock		*crf6* H_2O_2/Mock		CRF6oe/Col-0		*crf6*/Col-0	
		Fold Change	**Adj. p-value**	**Fold Change**	**Adj. p-value**	**Fold Change**	**Adj. p-value**	**Fold Change**	**Adj. p-value**
At1g03070	---	4.087	0.000614	2.021	0.125643	0.745159	0.283161	0.969105	0.994996
At1g05575	---	4.502	0.001429	1.749	0.269116	2.98596	5.12E-05	0.914665	0.97213
At1g05675	---	13.079	1.48E-05	6.071	1.17E-05	1.569696	0.232403	0.628707	0.531569
At1g05680	UGT74E2	8.847	2.00E-06	3.200	0.002694	1.188202	0.45074	1.124361	0.934461
At1g07160	---	4.213	0.002312	1.529	0.447808	1.394028	0.156764	1.226553	0.747377
At1g09500	---	6.669	0.000918	2.400	0.096716	2.79792	0.010122	0.858601	0.955252
At1g17170	GSTU24	27.295	1.67E-09	13.400	4.67E-08	2.233653	0.008677	1.112427	0.963099
At1g28480	GRX480	3.828	0.005106	1.810	0.109141	2.049639	0.01009	1.161742	0.918619
At1g54050	---	8.376	2.40E-07	3.164	0.000245	0.641511	0.11875	1.199198	0.88313
At1g56240	PP2-B13	15.291	8.49E-07	6.383	2.84E-06	1.433906	0.126194	0.908762	0.943674
At1g59860	---	5.623	7.64E-05	2.708	0.001656	2.297134	0.002947	0.95089	0.986676
At1g64950	CYP89A5	5.910	9.19E-05	1.694	0.315712	1.753582	0.064667	1.229754	0.895368
At1g65490	---	4.771	0.00053	2.179	0.083004	2.790986	0.034586	0.754342	0.813278
At1g65790	RK1	4.058	0.000711	1.174	0.867683	0.572061	0.144183	1.105256	0.964688
At1g66570	SUC7	9.844	2.23E-05	3.323	0.036745	0.745213	0.353946	0.962551	0.988659
At1g71520	---	11.644	2.68E-07	4.371	1.10E-05	3.499309	0.000474	0.909806	0.945899
At1g73120	---	2.464	0.006099	1.132	0.921862	2.115781	0.001037	1.079123	0.971878
At1g76600	---	8.184	2.77E-06	4.021	5.62E-05	1.347813	0.337194	0.768912	0.690988
At2g02930	GSTF3	3.351	0.01339	1.432	0.632801	4.420976	0.00018	1.132154	0.962977
At2g18660	PNP-A	7.031	6.59E-05	2.475	0.117142	0.902798	0.787152	1.863649	0.523989
At2g19310	---	2.326	0.018839	1.137	0.80123	3.619311	1.83E-05	1.997748	0.039703
At2g20560	---	3.599	0.006777	1.684	0.190636	1.401625	0.268885	1.047235	0.986351
At2g25510	---	4.001	2.87E-05	1.794	0.250035	2.490119	6.63E-05	2.389684	0.043263
At2g31945	---	4.308	0.016834	2.073	0.111781	3.287019	5.53E-05	0.775538	0.786758
At2g42530	COR15B	2.872	0.033637	1.395	0.068141	0.222024	0.000198	3.553313	0.006258
At2g42540	COR15A	5.023	4.74E-06	1.738	0.000741	0.529624	0.002381	4.22964	2.48E-07
At3g16030	CES101	2.376	0.011976	0.889	0.930823	0.461466	0.002221	1.201424	0.862305
At3g16050	PDX1.2	2.805	0.001067	1.319	0.349888	1.279101	0.267407	1.162636	0.82232
At3g25010	RLP41	2.583	0.002212	1.285	0.874394	0.508736	0.08861	1.31911	0.900542
At3g46080	---	5.347	0.000511	2.666	0.000689	3.178597	0.000347	0.924458	0.973011
At3g47090	---	3.175	0.006022	1.556	0.529003	1.117574	0.739698	1.142429	0.908146
At3g56710	SIB1	6.166	0.003203	2.651	0.002748	1.282537	0.558818	1.146559	0.953794
At4g08555	---	8.309	0.000107	2.763	0.001425	1.201732	0.547516	0.817112	0.676432
At4g12400	HOP3	10.056	1.17E-05	4.944	2.96E-05	1.659899	0.163413	1.110558	0.97199
At4g14400	ACD6	4.841	2.60E-06	2.131	0.046115	0.38226	0.026489	2.700815	0.015467

At4g34131	UGT73B3	6.369	9.35E-05	2.707	0.002293	1.740691	0.142685	1.298958	0.789332
At5g12020	HSP17.6II	43.879	1.22E-08	14.813	5.01E-09	1.409804	0.37696	1.192736	0.911474
At5g22140	---	14.377	1.53E-07	5.077	1.75E-06	0.746503	0.456183	1.156812	0.919569
At5g24110	WRKY30	4.709	0.001709	2.265	0.029944	1.422743	0.359308	0.954916	0.98892
At5g24150	SQP1	3.327	0.001278	1.487	0.539497	2.144037	0.012205	1.002787	0.999186
At5g26170	WRKY50	2.445	0.044762	0.981	0.995677	1.276838	0.540037	1.791024	0.374908
At5g37260	RVE2	2.459	0.028522	0.853	0.869761	6.875764	2.77E-07	3.759967	0.004782
At5g37670	---	3.936	0.0024	1.291	0.783856	0.840442	0.61076	1.379093	0.722411
At5g39090	---	3.217	0.00212	1.306	0.675673	1.114043	0.798373	0.978657	0.994996
At5g48850	ATSDI1	2.844	0.002406	1.054	0.989779	0.496447	0.016463	5.181519	0.000129
At5g54165	---	25.096	3.84E-08	7.748	4.31E-07	19.86539	9.75E-10	1.36924	0.731665
At5g54610	ANK	2.786	0.020643	1.149	0.957144	0.8377	0.604483	1.602012	0.693988
At5g59310	LTP4	5.808	0.002223	1.041	0.992717	2.102455	0.064062	1.825871	0.499735
At5g59320	LTP3	9.812	1.49E-07	1.644	0.409198	1.28915	0.504588	1.717964	0.411951

Supplementary Table 2. Expression of CRF6-dependent-repressed genes.

Locus ID	Gene Symbol	Col-0 H_2O_2/Mock		*crf6* H_2O_2/Mock		CRF6oe/Col-0		*crf6*/Col-0	
		Fold Change	**Adj. p-value**	**Fold Change**	**Adj. p-value**	**Fold Change**	**Adj. p-value**	**Fold Change**	**Adj. p-value**
At1g02810	---	0.441578	0.046409	0.670486	0.177772	0.8349085	0.5466505	0.8994344	0.9257
At1g12040	LRX1	0.211628	6.59E-05	0.480203	0.037065	2.69541	0.0001131	0.7306463	0.5873
At1g13480	DUF1262	0.226882	0.00028	0.601931	0.254036	1.828309	0.0044716	0.620589	0.2622
At1g18860	WRKY61	0.184839	2.42E-05	0.299275	6.96E-05	1.015475	0.9580303	0.797408	0.5384
At1g20900	ESC	0.484922	0.033229	0.775213	0.566536	1.159168	0.6133178	0.6467836	0.113
At1g26250	---	0.102532	1.36E-07	0.219961	3.24E-06	1.544291	0.0453885	1.804576	0.0488
At1g33750	---	0.342118	0.018269	0.577173	0.394614	0.6273533	1.63E-01	0.8114871	0.9035
At1g44160	---	0.431574	0.040388	0.648294	0.440378	0.6109093	0.0957137	0.8364986	0.902
At1g51850	---	0.080043	2.81E-05	0.129188	1.79E-06	0.6639999	0.142795	0.6348026	0.4862
At1g60960	IRT3	0.388766	0.010548	0.612561	0.159005	0.7506774	0.1691606	0.948211	0.972
At1g73300	scpl2	0.255773	0.001286	0.526775	0.417253	1.341033	0.3657201	0.3673711	0.08
At1g80240	DGR1	0.276552	0.001278	0.474957	0.001257	0.9959257	0.9919067	0.8391089	0.7846
At2g05510	---	0.422936	0.01006	0.718545	0.09317	1.152678	5.19E-01	0.9922393	0.9992
At2g18370	---	0.445785	0.007074	0.753182	0.268221	0.9702578	0.9150813	0.9965783	0.9992
At2g19190	FRK1	0.321869	0.031979	0.601351	0.383704	0.5142404	0.0328332	0.3926117	0.081
At2g30840	---	0.265834	0.000833	0.565116	0.104695	0.6518198	0.1188472	0.726032	0.4579

At2g38940	PHT1;4	0.287895	0.012516	0.472215	0.077865	0.9235199	0.8559113	0.7071705	0.7669
At2g42060	---	0.308532	0.005001	0.487955	0.098507	0.5326446	0.0600084	0.6172963	0.4922
At2g46740	GOLLU5	0.23428	0.000512	0.415196	0.006517	2.267252	0.0065537	0.8266938	0.7708
At2g46750	GULLO2	0.176999	1.44E-05	0.37878	0.000918	2.144647	0.0010606	0.7019937	0.2465
At2g47540	---	0.326007	0.034135	0.50242	0.073038	0.5931833	0.1317369	0.8176328	0.902
At2g47550	---	0.499861	0.022094	0.922736	0.936734	1.133324	0.6098896	0.6851539	0.2478
At3g01420	DOX1	0.097591	3.61E-07	0.168722	1.79E-09	1.187021	0.4632241	0.9929239	0.9992
At3g12977	---	0.321663	0.003375	0.544551	0.106145	1.147994	0.7177352	0.8752093	0.9408
At3g13403	---	0.31387	0.003343	0.774343	0.807947	0.7791781	0.3972265	0.5912458	0.3043
At3g13760	---	0.299778	0.009689	0.508354	0.007834	0.6840957	0.1941138	0.7823223	0.6855
At3g16770	EBP	0.41285	0.004758	0.74856	0.42847	2.565331	5.38E-05	0.8240507	0.7368
At3g21351	---	0.356267	0.004758	0.616272	0.413347	2.781783	2.75E-05	0.5634775	0.2067
At3g21510	AHP1	0.383179	0.011158	0.657528	0.207698	1.846201	0.0055052	7.69E-01	0.5538
At3g22800	---	0.34746	0.039238	0.730393	0.56925	1.452552	0.1505651	0.7221323	0.584
At3g23125	---	0.478934	0.049518	1.14254	0.938685	1.03967	0.9374664	0.8130241	0.9074
At3g28550	---	0.10792	0.000109	0.162075	1.41E-07	5.084056	8.57E-06	1.074474	0.9771
At3g55090	ABCG16	0.352622	0.00668	0.676527	0.677186	0.6028016	0.0780667	0.6750705	0.5947
At4g11650	OSM34	0.15065	2.04E-06	0.234222	3.57E-08	3.61906	5.74E-07	1.454154	0.1304
At4g12090	---	0.455408	0.013273	0.683671	0.274267	1.760378	0.0050014	0.7283531	0.3895
At4g12470	AZI1	0.196618	0.001015	0.652792	0.486316	1.313713	4.81E-01	0.576483	0.565
At4g12480	EARLI1	0.287914	0.000883	0.881499	0.928204	4.537649	1.05E-06	0.5236573	0.2426
At4g13280	TPS12	0.451656	0.02037	0.705054	0.553149	0.6414261	1.13E-01	0.8132242	0.8404
At4g13300	TPS13	0.236941	0.000719	0.783812	0.73812	3.687952	0.0003237	0.4623236	0.0641
At4g14630	GLP9	0.157695	1.61E-05	0.25815	2.24E-06	0.7367311	0.1254133	0.8693476	0.7893
At4g20362	---	0.364083	0.016707	0.728166	0.697656	3.165449	0.0003465	0.6155871	0.5094
At4g22610	---	0.361105	0.024606	0.627316	0.124936	2.893529	0.0012166	0.5908976	0.3191
At4g22810	---	0.437147	0.025555	1.034573	0.991285	0.5863707	5.21E-02	0.7569264	0.7569
At4g24310	DUF679	0.263581	0.000359	0.40745	0.012035	1.262803	0.3425053	0.9374671	0.972
At4g28720	YUC8	0.385445	0.028314	0.602321	0.195387	0.9212854	7.83E-01	7.98E-01	0.7726
At4g36570	RL3	0.430624	0.035423	0.71707	0.424734	0.5640891	0.115356	0.9742609	0.992
At4g38080	---	0.36724	0.005424	0.562202	0.008362	1.250946	0.2221812	0.6574007	0.0809
At4g38780	---	0.322422	0.029371	0.989482	0.998744	1.038622	9.20E-01	0.8084273	0.7877
At4g40010	SNRK2.7	0.379396	0.039666	0.654434	0.448085	1.336181	2.54E-01	1.18E+00	0.825
At5g05500	MOP10	0.456379	0.015003	0.716921	0.51875	1.495751	0.1000946	0.6912694	0.557
At5g19520	MSL9	0.366861	0.003758	0.657127	0.179768	0.7450789	0.2744474	0.8851078	0.908
At5g19890	---	0.129261	7.23E-06	0.390443	0.001041	2.601475	0.0004200	0.761906	0.4684
At5g35190	EXT13	0.155533	0.000268	0.299434	0.000536	1.898184	0.0197065	0.5602198	0.102
At5g43580	UPI	0.19404	0.00028	0.300082	0.000671	3.996356	5.61E-07	0.6963744	0.4013
At5g44610	MAP18	0.316168	0.04136	0.519905	0.10939	0.6194952	0.1150847	0.6209031	0.5103
At5g66870	ASL1	0.301691	0.002264	0.517376	0.077865	0.8768671	0.6696597	0.9045768	0.9322
At4g22470	---	0.176948	0.000681	0.458531	0.101147	6.70915	3.65E-08	0.3118275	0.0121
At5g55050	---	0.427549	0.001182	0.67219	0.209208	1.7117	0.0035046	0.5643766	0.0409
At1g07560	---	0.172526	1.23E-05	0.323289	0.000722	0.3801406	0.0019005	0.7726115	0.734

At1g08090	NRT2:1	0.087416	3.07E-06	0.184781	5.51E-07	0.1362176	3.10E-08	0.9291929	0.9487
At1g12740	CYP87A2	0.340241	0.026451	0.607615	0.174888	0.4246644	0.0026046	0.8896779	0.9181
At1g30280	---	0.444677	0.006106	0.712791	0.175845	0.1412209	9.00E-07	0.7926962	0.4071
At1g31770	ABCG14	0.266095	0.001735	0.438516	0.000772	0.3932722	0.0002041	0.8687662	0.8294
At1g49860	GSTF14	0.092764	3.34E-07	0.204124	0.000778	0.1531455	1.49E-07	0.958347	0.9889
At1g49960	---	0.283149	0.00584	0.513012	0.006943	0.4991672	0.0055050	0.6884577	0.374
At1g52450	---	0.3601	0.023804	1.106739	0.941671	0.4219898	0.0041327	0.5982975	0.2424
At1g53610	---	0.302291	0.000745	0.565669	0.115286	0.5569057	4.76E-02	0.6018559	0.3478
At1g64920	---	0.381061	0.020067	0.789108	0.834358	0.3441156	0.0002105	0.7263793	0.7339
At1g67710	ARR11	0.359651	0.003384	0.662368	0.386545	0.5239133	0.0036477	0.650459	0.1632
At1g71380	CEL3	0.251193	0.000314	0.401594	0.008189	0.3656246	0.0006712	0.5059494	0.1044
At1g78000	SULTR1;2	0.391363	0.00084	0.590396	0.021154	0.5630735	0.0052539	0.7609771	0.4557
At2g21045	---	0.157122	0.000296	0.273946	2.27E-05	0.5545713	0.0048947	1.216743	0.6471
At2g23540	---	0.275745	0.000136	0.448964	0.000171	0.2938639	4.79E-06	0.8165058	0.6429
At2g35770	scpl28	0.233414	0.000652	0.395805	9.46E-05	0.5589922	2.27E-02	0.9593472	0.9854
At2g37280	PDR5	0.484789	0.012315	0.744465	0.513751	0.3638738	0.0001621	0.8654666	0.8326
At3g02850	SKOR	0.357237	0.04412	0.538557	0.259018	0.4395076	0.0237796	0.8411646	0.9074
At3g13610	---	0.401894	0.013065	0.638266	0.07611	0.4772113	1.26E-02	0.9828206	0.9957
At3g20380	---	0.086001	1.02E-07	0.16778	1.20E-05	0.3935626	0.0058913	0.7969052	0.7339
At3g22770	---	0.391359	0.022723	1.566565	0.454912	0.4547892	0.0056677	0.5810221	0.2799
At3g46330	MEE39	0.274782	0.001562	0.441788	0.077281	0.2714334	3.45E-05	0.6278949	0.5103
At3g54040	---	0.110521	2.20E-07	0.214725	6.82E-07	0.5165035	0.0007331	0.9148836	0.9273
At3g57040	ARR9	0.445712	0.011147	0.775068	0.593974	0.2799896	0.0005477	0.4996051	0.0182
At4g28410	---	0.313058	0.001278	0.536586	0.040873	0.3578533	0.0050261	0.7088587	0.4073
At4g30170	---	0.124939	2.77E-06	0.201803	4.37E-08	0.5638116	0.0036705	1.0532	0.968
At4g37070	PLP1	0.260217	0.000562	0.524838	0.177817	0.4918925	0.0261564	0.4440318	0.1318
At5g02360	---	0.233377	0.001138	0.399898	0.124384	0.3783216	0.0027364	0.6640643	0.3977
At5g05880	---	0.314507	0.004758	0.473242	0.121163	0.4672317	0.0089124	1.05862	0.9856
At5g06090	GPAT7	0.239559	0.006542	0.37665	0.003164	0.5244565	0.0125289	0.8935652	0.927
At5g06300	LOG7	0.484885	0.02315	0.740476	0.125643	0.3677265	0.0001173	0.6562375	0.1354
At5g13580	---	0.375926	0.022623	0.615602	0.195445	0.5232419	1.20E-02	0.7698264	0.5942
At5g22550	DUF247	0.424329	0.043649	0.713198	0.511257	0.3306393	8.22E-05	0.6461787	0.2779
At5g25110	CIPK25	0.268925	0.004461	0.509146	0.152105	0.4607002	0.0090325	7.60E-01	0.7685
At5g40510	---	0.265064	0.000455	0.480131	0.074172	0.519905	0.0115638	0.8697605	0.8831
At5g43350	PHT1;1	0.13528	1.06E-05	0.2387	2.50E-06	0.5173025	2.28E-02	0.9990578	0.9995
At5g43520	---	0.202365	6.55E-05	0.430027	0.02319	0.2407537	1.48E-06	0.5705202	0.0574
At5g62920	ARR6	0.386025	0.017458	0.731247	0.732309	0.3612864	0.0013049	0.4172286	0.0856
At5g64100	---	0.249662	0.000203	0.449512	6.69E-05	0.6121491	0.0181592	0.7483681	0.2604
At5g65790	MYB68	0.36694	0.003809	0.809484	0.803889	0.4084963	0.0003464	0.6248232	0.1965

Supplementary Table 3. Expression of genes showing enhanced regulation in the absence of CRF6.

Locus ID	Gene Symbol	Col-0 H_2O_2/Mock		*crf6*[2] H_2O_2/Mock		CRF6oe/Col-0	
		Fold Change	**Adj. p-value**	**Fold Change**	**Adj. p-value**	**Fold Change**	**Adj. p-value**
At1g69930	GSTU11	5.675	0.001856	8.612	4.03E-06	4.499423	5.97E-05
At5g52050	---	2.975	0.014071	4.579	2.25E-05	4.327623	0.000924
At1g15415	---	2.359	0.009955	3.814	0.00017	3.8199	5.63E-06
At1g02850	BGLU11	3.326	0.000227	5.972	1.08E-06	3.126601	8.01E-06
At3g15356	---	2.830	0.002025	7.372	3.63E-08	2.802559	0.000318
At4g17490	ERF6	2.688	0.046037	5.440	4.03E-05	2.681388	0.000124
At1g02930	GSTF6	2.665	0.006381	4.504	4.57E-07	2.347467	0.0002
At3g09405	---	3.362	0.001239	5.793	1.70E-07	2.16214	0.001752
At5g64750	ABR1	3.175	0.001202	5.538	3.08E-06	1.911175	0.043546
At3g16530	---	3.516	0.000104	6.995	2.91E-08	1.911122	0.001305
At2g44460	BGLU28	8.917	1.25E-05	15.261	3.21E-05	1.355063	0.296776
At4g21680	NRT1.8	3.913	0.000123	11.351	7.07E-09	1.248512	0.558818
At4g33930	---	2.515	0.004063	5.224	5.59E-06	1.106244	0.765562
At1g69920	GSTU12	3.921	0.000732	6.536	1.41E-07	0.841162	0.605448
At2g04040	---	2.310	0.009801	7.453	9.49E-07	0.802918	0.379752
At2g15780	---	2.645	0.030692	4.010	1.34E-05	0.776445	0.48111
At3g26830	PAD3	4.591	7.76E-05	10.467	2.30E-07	0.679575	0.127008
At4g32950	---	0.23666	0.000168	0.0974	4.91E-08	0.3921629	0.001398
At1g47600	BGLU34	0.22953	0.00122	0.096457	5.34E-08	0.8953633	0.756446
At5g14650	---	0.36848	0.036558	0.163355	4.95E-08	0.5190786	0.024597